SANDIA REPORT
SAND2000-0771
Unlimited Release
Printed February 2001

Predictive Modeling of MIU3-MIU2 Interference Tests: MIU Site, Toki, Japan

Sean A. McKenna and Randall M. Roberts

Prepared by
Sandia National Laboratories
Albuquerque, New Mexico 87185 and Livermore, California 94550

Sandia is a multiprogram laboratory operated by Sandia Corporation, a Lockheed Martin Company, for the United States Department of Energy under Contract DE-AC04-94AL85000.

Sandia National Laboratories

Issued by Sandia National Laboratories, operated for the United States Department of Energy by Sandia Corporation.

Available to DOE and DOE contractors from
U.S. Department of Energy
Office of Scientific and Technical Information
P.O. Box 62
Oak Ridge, TN 37831

Telephone: (865)576-8401
Facsimile: (865)576-5728
E-Mail: reports@adonis.osti.gov
Online ordering: http://www.doe.gov/bridge

Available to the public from
U.S. Department of Commerce
National Technical Information Service
5285 Port Royal Rd
Springfield, VA 22161

Telephone: (800)553-6847
Facsimile: (703)605-6900
E-Mail: orders@ntis.fedworld.gov
Online order: http://www.ntis.gov/ordering.htm

SAND2000-0771
Unlimited Release
Printed February 2001

Predictive Modeling of MIU3-MIU2 Interference Tests:

MIU Site, Toki, Japan

Sean A. McKenna and Randall M. Roberts
Sandia National Laboratories
PO Box 5800
Albuquerque, New Mexico 87185-0735

Abstract

Predictive modeling of the results of a series of interference tests being conducted at the MIU site in central Japan are conducted using a well -test simulator (n-SIGHTS) developed at Sandia National Laboratories. A Monte Carlos approach is used to acknowledge uncertainty in the values of hydraulic conductivity, specific storage and flowpath length. The Monte Carlo results provide a distribution of possible values for the time to 1 meter of observed drawdown and the total amount of drawdown after 12 days of pumping. Each of these two results is calculated for each of six observation locations in and around the Tsukyoshi fault. A total of 500 realizations of the interference test for each of two different conceptual models are examined. The radial flow, or Theis, conceptual model results show that none of the realizations produce more than one meter of drawdown in any of the six observation piezometers. The second conceptual model considers the flow dimension to also be a stochastic parameter with a uniform distribution between 1 (linear flow) and 2 (radial flow). These results indicate that for the model setup employed in this study it is necessary to have a flow dimension less than or equal to approximately 1.9 in order to achieve more than one meter of drawdown in any of the observation parameters. A simple sensitivity analysis shows that the amount of drawdown occurring after 12 days of pumping is most sensitive to the flow dimension and nearly independent of the specific storage value.

Acknowledgements

This report benefited from thoughtful reviews by Shinji Takeuchi, Hiromitsu Saegusa, Katsushi Nakano, Susan Altman and Erik Webb. This work was funded by the Japan Nuclear Cycle Development Institute through a contract with Sandia National Laboratories. Sandia is a multiprogram laboratory operated by Sandia Corporation, a Lockheed Martin Company, for the United States Department of Energy under Contract DE-AC04-94AL85000.

Table of Contents

List of Figures

List of Tables

Introduction

JNC is planning a series of interference tests between the MIU-3 and MIU-2 boreholes at the MIU site. In order to predict the success of these tests, Sandia National Laboratories has conducted probabilistic modeling of the interference tests. The approach taken in this probabilistic modeling and the results of the modeling are given in this report.

The goal of this project is to predict the drawdown that will be observed in specific piezometers placed in the MIU-2 borehole due to pumping at a single location in the MIU-3 borehole. These predictions are in the form of distributions obtained through multiple forward runs of a well-test model. Specifically, two distributions will be created for each pumping location--piezometer location pair: 1) the distribution of the times to 1.0 meter of drawdown and 2) the distribution of the drawdown predicted after12 days of pumping at a discharge rates of 25, 50, 75 and 100 *l*/hr. Each of the steps in the pumping rate lasts for 3 days (259,200 seconds). This report is based on results that were presented at the Tono Geoscience Center on January 27th, 2000, which was approximately one week prior to the beginning of the interference tests.

Hydraulic conductivity (K), specific storage (S_s) and the length of the pathway (L_p) are the input parameters to the well-test analysis model. Specific values of these input parameters are uncertain. This parameter uncertainty is accounted for in the modeling by drawing individual parameter values from distributions defined for each input parameter. For the initial set of runs, the fracture system is assumed to behave as an infinite, homogeneous, isotropic aquifer. These assumptions correspond to conceptualizing the aquifer as having Theis behavior and producing radial flow to the pumping well.

A second conceptual model is also used in the drawdown calculations. This conceptual model considers that the fracture system may cause groundwater to move to the pumping well in a more linear (non-radial) manner. The effect of this conceptual model on the drawdown values are examined by casting the flow dimension (F_d) of the fracture pathways as an uncertain variable between 1.0 (purely linear flow) and 2.0 (completely radial flow.

Available Data

The JNC site characterization team at the Tono Geoscience Center (Takeuchi, written communication) has provided information regarding the hydraulic properties of fracture zones in the vicinity of the MIU site. The fractured-rock data provided include 208 measurements of hydraulic conductivity and 7 measurements of specific storage.

In addition to the hydraulic information, the placement of the pumping location in the MIU-3 borehole and the locations of the six packed intervals in the MIU-2 borehole have been provided. The locations of the pumping interval and the piezometers are shown in Figure 1. The straight-line distance between the MIU-2 and MIU-3 boreholes is 134.5 meters.

The depth below ground to the top and bottom of the receiver sections (the MP intervals) within MIU-2 and the injection/withdrawal section in MIU-3 were provided by the TGC staff. These depths were converted to elevations above mean sea level for this exercise. The locations given as both depth below ground level and elevation are shown in Table 1. The elevations at the top of MIU-2 and MIU-3 respectively are: 223.8 and 230.5 meters above sea level. A schematic diagram of the pumping interval, the Tsukyoshi Fault and the MP locations is provided in Figure 1. The boundaries of the Tsukyoshi Fault in Figure 1 are approximate and both the low permeability fault core and some of the high permeability damage zone around the fault core are included within these boundaries.

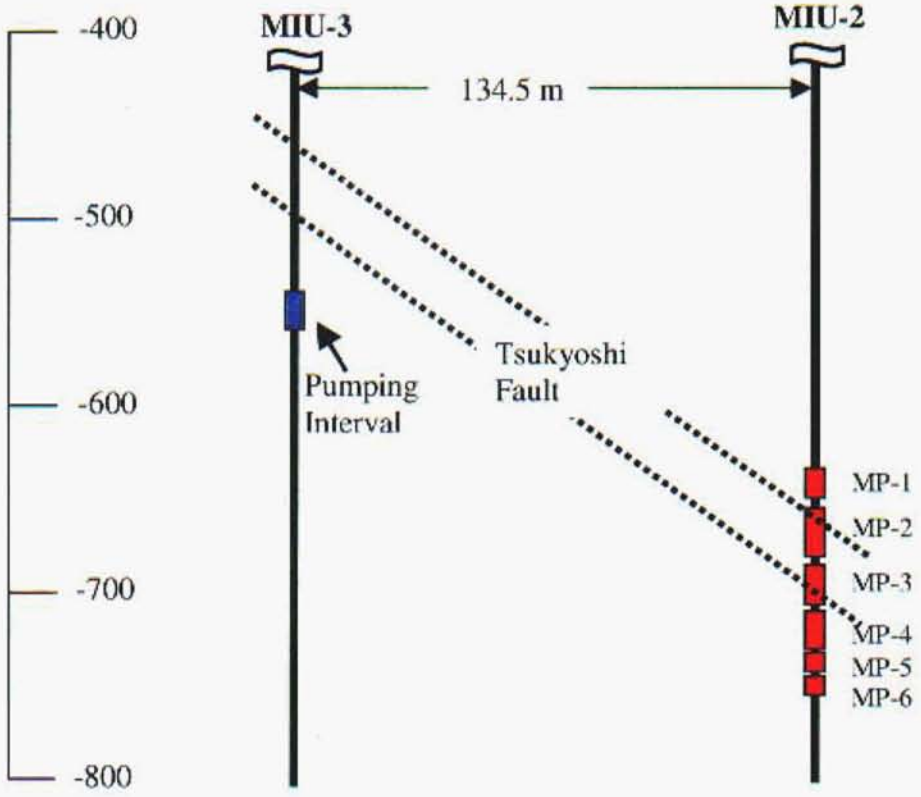

Figure 1. Cross-sectional schematic view of the pumping interval and piezometer locations in the MIU-3 and MIU-2 boreholes. Elevations are given in meters above sea level. The scale on the left side of the figure is elevation in meters. Note that the full length of the boreholes is not shown here.

Table 1. Depths and elevations of intervals in the MIU-2 and MIU-3 boreholes.

Interval	Depth to Top of Interval (m)	Depth to Bottom of Interval (m)	Top Elevation (m)	Bottom Elevation (m)
Withdrawal MIU-3	777	802	-546.5	-559
MP-1	868	885	-644.7	-661.2
MP-2	888	916	-664.7	-692.2
MP-3	917	931	-693.7	-707.2
MP-4	932	959	-708.7	-735.2
MP-5	960	971	-736.7	-747.2
MP-6	972	983	-748.7	-759.2
Tsukyoshi Fault MIU-2	888	916	-664.7	-692.2
Tsukyoshi Fault MIU-3	698	723	-467.5	-492.5

Uncertainty in Input Parameters

The values of K and S_s are not known across the specific fracture pathways being tested. These parameters are only known in a statistical sense by inference from packer tests conducted at other locations both within and nearby the MIU site. The exact length of the fracture path between the pumping interval and the specific piezometer location is also unknown. At a minimum, this distance must be at least as long as the straight-line distance between the pumping interval and each piezometer location.

Uncertainty in the exact values of drawdown in MIU-2 due to pumping in the MIU-3 borehole is modeled by employing a Monte Carlo modeling approach. A total of 500 possible values of the log10 K and log10 S_s parameters are drawn, independently, from distributions describing the uncertainty in these parameters. Distributions defining the uncertainty in these parameters are constructed by fitting analytical distributions to the available data. The parameters defining these fitted distributions are shown in Table 2 and the analytical distributions are compared to the available data in Figure 2.

Table 2. Parameters defining the distributions fit to the K and S_s data provided by JNC.

Parameter	**Log10 K (m/s)**	**Log10 Ss (1/m)**
Distribution	Normal	Uniform
Number of Data	208	7
Minimum	NA	-11.5
Maximum	NA	-6.5
Mean	-8.19	-9.0
Standard Deviation	1.66	1.4
Median	-8.19	-9.0

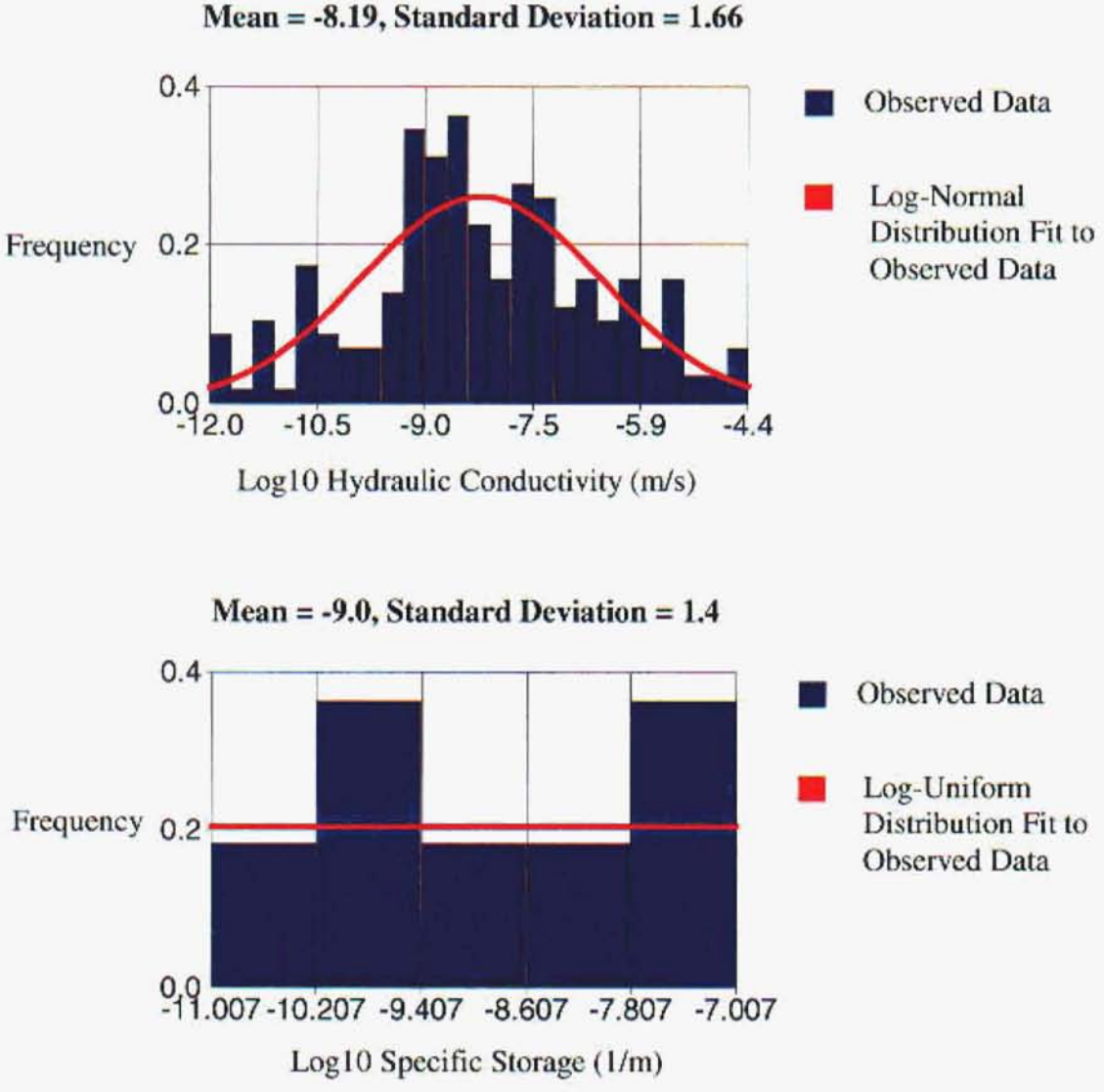

Figure 2. Distributions of log10 transformed hydraulic conductivity (upper image) and specific storage (lower image). The actual data are shown in blue and the fitted distributions are shown in red. The mean and standard deviation of the distributions are indicated in the titles above the graphs.

It is noted that uncertainty in the values of K and S_s is also due to the interpretation of the individual slug tests. For example, the values shown in Figure 2 are based on an assumption of radial flow to the test interval. Another possible interpretation could be made under the assumption of non-radial flow to the test interval (e.g., the variable flow dimension case discussed below). This type of uncertainty arising from the test interpretation is not considered further in this study.

The third uncertain parameter to be modeled in this predictive exercise is the path length, L_p, between the pumping location in MIU-3 and each piezometer in MIU-2. There are no quantitative data on the possible distributions of path lengths through the fracture system. However, it is possible to use simple geometric arguments to determine the minimum possible path length between each pumping location and the piezometer locations. These minimum path lengths are given for each piezometer in Table 3.

The distribution of L_p is defined using the minimum possible path length and some assumptions regarding the connectivity of the fracture system. It is assumed that the minimum *actual* path length is one percent longer than the minimum *possible* path length. The most likely actual path length is assumed to be 20 percent longer than the minimum possible path length and the largest actual path length is assumed to be 60 percent longer than the minimum possible path length. These values correspond to tortuosities of 1.01, 1.20 and 1.60 along the flow paths. There are no data available from the MIU site to support these assumptions. These values are based solely on expert judgement. For each piezometer, the minimum, most likely and maximum path lengths are defined in Table 3. These three values are used as the parameters that define a triangular distribution of path lengths for each piezometer.

Table 3. Minimum fracture path lengths, L_p, and parameters defining the triangular distributions of path lengths.

Piezometer	Minimum Possible Path Length (m)	Minimum Actual Path Length (m)	Most Likely Actual Path Length (m)	Maximum Actual Path Length (m)
MP-1	163.9	165.6	196.7	262.3
MP-2	179.7	181.5	215.7	287.6
MP-3	195.0	197.0	234.0	312.1
MP-4	210.7	212.9	252.9	337.2
MP-5	226.9	229.2	272.3	363.0
MP-6	236.7	239.0	284.0	378.7

Modifications to Input Parameters

The S_s values shown in Figure 2 and described in Table 2 are extremely low values. There are only seven measurements of specific storage, all made in the same borehole, and they range from $9.9E^{-12}$ to $9.9E^{-08}$ (1/m). These values are extremely small, even for fractured rocks. It is possible that these results may be caused by a skin effect around the

borehole. If these values are used in the prediction of drawdown in the MIU-2 borehole from pumping in the MIU-3 borehole, the pressure front reaches the MIU-2 borehole in less than 1 second. Therefore, some additional examination of these values was necessary.

Specific storage is calculated as:

$$S_s = \rho_w g(\beta_p + \phi\beta_w)$$

where ρ_w is the density of water [kg/m^3], g is gravitational acceleration [m/sec^2], β_p is the compressibility of the rock [m^2/N], ϕ is the porosity of the rock[-] and β_w is the compressibility of water [m^2/N]. The range of compressibilities measured on fractured rocks range from 3.3E^{-10} to 6.9E^{-10} m^2/N (Domenico and Schwartz, 1990, Table 4.1). The compressibility of water at 25 degrees C is 4.8E-10 m^2/N (Domenico and Schwartz, 1990, page 105).

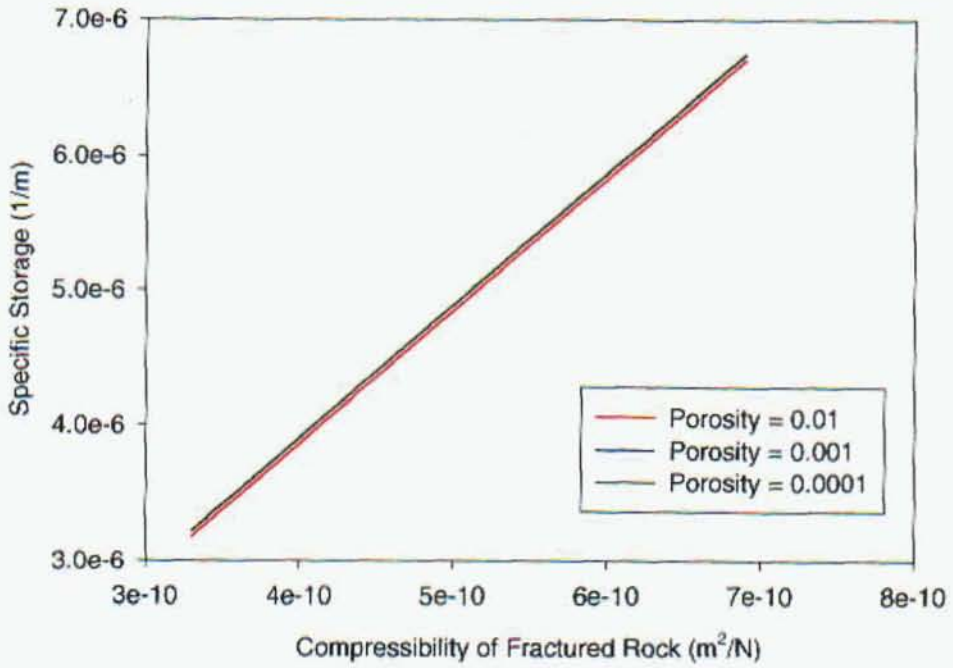

Figure 3. Plot showing specific storage as a function of rock compressibility for three different values of porosity.

A series of calculations of S_s are made across the range of possible rock compressibility values for three different fracture porosities: 0.01, 0.001, and 0.0001. In these calculations, the density of water is assumed to be 997 kg/m^3 and gravitational acceleration is set to 9.81 m/sec^2. The results of these calculations are shown in Figure 3.

The values of specific storage from these calculations suggest a range of specific storage is approximately from 3.0E^{-06} to 7.0E^{-06} (1/m). These values are considerably higher (2 to 6 orders of magnitude) than those measured in MIU-1, and the range of values is much

narrower (less than one-half an order of magnitude). The results in Figure 3 also show that the assumed fracture porosity has only a small effect on the calculated value of specific storage.

The S_s values measured in MIU-1 appear to be smaller than physically possible. In order to make meaningful predictions of drawdown at MIU-2, we propose that a uniform distribution of S_s values between $3.0E^{-06}$ to $7.0E^{-06}$ (1/m) applies to this problem. Specific storage values are taken from this proposed distribution for the drawdown calculations given in this report.

The distribution for hydraulic conductivity is modified to have a standard deviation less than what was observed in the actual measured values. This modification is done by decreasing the standard deviation of the distribution by a factor of 2.0. This new standard deviation is 0.83 compared to 1.66 in the original distribution. The standard deviation of the hydraulic conductivity values is reduced in order to account for the scale difference between the hydraulic conductivity measured in the slug tests (small scale) and the effective, or average, hydraulic conductivity of the pathways between the pumping interval in MIU-3 and the MP's in MIU-2 (large scale). The actual scale difference and the scaling process are unknown and this reduction in variability is based solely on expert judgement. The mean of the lognormal distribution remains the same as the measured distribution (-8.19).

Input Vectors

Distributions for the three critical parameters (K, S_s, L_p) governing the amount of drawdown in an interference test have been derived. These distributions are based on a large amount of data (hydraulic conductivity), published values (specific storage) and a lower limit on the possible values coupled with some assumptions on the shape of the distribution (path length). Prior to running the forward models of the interference test in the well-test analysis code, it is necessary to draw a set of input vectors from these distributions.

Each forward run of the well-test analysis code requires a value of K, S_s and L_p drawn from the distributions defined above. A single value of each of these three parameters comprises an *input vector*. In this exercise, a total of 500 input vectors are drawn from the distributions. The 500 values of K and S_s are kept the same for each piezometer as those distributions are based on data that are considered to be regionally applicable in the vicinity of the MIU site. These 500 K and 500 S_s values are drawn from the log-normal and uniform distributions defined above.

The path length distributions defined in Table 3 are specific for each different piezometer. Therefore, 500 different values of L_p are drawn for each piezometer for a total of 3000 different path length values. The parameters summarizing the K, S_s and L_p vectors are given in Table 4. The distributions summarized in Table 4 are from the actual parameter values used in the simulations presented here. There are 500 values in each distribution.

Flow Dimension

Well-test analysis methods used to estimate K and S_s were historically developed to characterize flow within idealized radial flow systems (left image, Figure 4), i.e., flow within a homogeneous, isotropic, constant-thickness porous medium. Flow within fractured hydrogeologic systems, however, can be quite different than flow within a homogeneous porous medium. Fractured systems tend to channelize the flow such that a few high permeability pathways supply water to a pumping well (right image, Figure 4). The flow dimension describes the flow pattern towards the pumping well, with fully radial flow having a dimension of 2.0, and flow in single, linear fracture having a dimension of 1.0. The concept of a flow dimension is added to this analysis to account for the complex and variable geometry that is often observed in fractured hydrogeologic systems.

Table 4. Statistical parameters of the input distributions of K, S_s and L_p used in the interference test model runs. There are 500 values in each distribution.

Vector	Mean	Standard Deviation	Median	Minimum	Maximum
Log10 K (m/s)	-8.19	0.83	-8.19	-10.96	-5.74
Log10 S_s (1/m)	-5.34	0.11	-5.34	-5.52	-5.16
MP-1 Length (m)	208.2	20.2	206.0	167.9	261.3
MP-2 Length (m)	228.3	22.1	225.8	183.9	286.5
MP-3 Length (m)	247.7	24.0	245.1	199.4	310.3
MP-4 Length (m)	267.7	25.9	264.8	215.1	333.8
MP-5 Length (m)	288.2	27.9	285.1	231.4	360.8
MP-6 Length (m)	300.6	29.1	297.4	240.0	374.2

Predictions of the time to 1.0 meter drawdown and the amount of drawdown after twelve days of pumping at each piezometer are also created for the case of uncertainty in the flow dimension. Information on the flow dimension of the fracture system for the subsurface at the MIU site has not been obtained. Therefore, uncertainty in the value of F_D is also handled through Monte Carlo modeling.

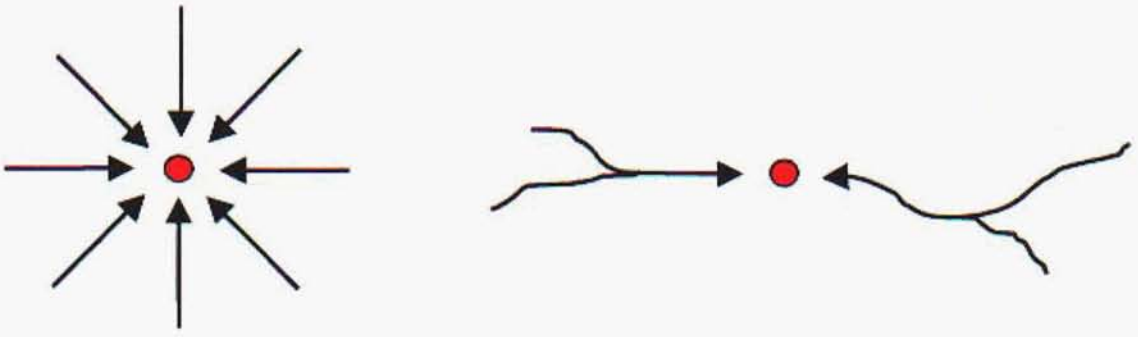

Figure 4. Schematic diagrams showing radial flow to a well (left) and channeled flow to a well (right). The flow dimension of the system in the left image is 2.0 and the flow dimension of the system in the right image is near 1.0

The case of flow dimension equal to 2.0 is the case of purely radial flow to a well in an isotropic, homogeneous, fully confined aquifer of infinite extent. This case is taken as the upper limit on the F_D distribution. The lower limit of the distribution is set to be 1.0 corresponding to the case of flow to a well that penetrates a one-dimensional (linear) fracture (see diagrams in Figure 4). A uniform distribution is assumed for the value of F_D between the lower and upper limits of 1.0 and 2.0.

A total of 500 values of F_D are drawn from the uniform distribution. The results of drawing these values are summarized in Table 5.

Table 5. Summary statistics of input distribution for flow dimension.

Mean	Standard Deviation	Median	Minimum	Maximum
1.50	0.29	1.50	1.00	2.00

Flow Modeling

Sandia National Laboratories, along with partner organizations in Canada, France, and Germany, is currently developing a numerical, MS-Windows-based well-test analysis code (*nSIGHTS*: n-dimensional, Statistical, Inverse, Graphical, Hydraulic Test Simulator). The code will have many special features designed to analyze tests performed in low permeability fractured systems, including the analysis of flow dimension, and the code will feature a full range of advanced statistical and probabilistic capabilities. A prototype version of *nSIGHTS* is employed in this study to calculate the drawdown distributions for both the radial and variable flow-dimension conceptual models. The *nSIGHTS* code provides a numerical implementation of analytical solutions for both radial and non-radial flow to, or from, wells.

The initial heads in each borehole are set to an arbitrarily large value within the model. This choice of initial head values may result in some large and unrealistic values of drawdown. However, this assumption does not affect the answer to the main question being asked: How long does it take to achieve 1 meter of drawdown.

The borehole diameter is also necessary as an input parameter. The caliper log for borehole MIU-3 was examined within the pumping interval (elevation -546 to -559 meters) and the average diameter was calculated to be 10.0 cm. This value is used for the borehole diameter within *nSIGHTS*. These models are run with stepped pumping rates for a total pumping time of 12 days. There are four steps, each lasting three days, and the pumping rates in these four steps are 25, 50, 75 and 100 liters/hour.

Model Results

Two sets, or ensembles, of realizations were run to predict the drawdown in MIU-2 from pumping in MIU-3. These two sets correspond to the fully radial (flow dimension = 2.0) and variable flow dimension cases as discussed above. The results of each set of models are described below.

Radial Conceptual Model

A total of 500 realizations were completed with the flow dimension set equal to 2.0. The head level in the pumping well was monitored to determine if the drawdown reached the pumping interval. It was assumed that if the drawdown in the pumping well exceeded 777 meters then the pumping well became dry. The 777-meter distance is the approximate distance from the ground surface to the top of the pumping interval in the pumping well

The results of these 500 forward models show that 105 of the 500 realizations resulted in more than 777 meters of drawdown in the pumping well (MIU-3). None of the remaining 395 realizations produced more than 1.00 meter of drawdown at any MIU-2 observation piezometer within the 12 day pumping period (Table 6). The maximum drawdown at the end of the 12-day pumping period across all pathways was 0.52 meters. Although, none of the realizations produced more than one meter of drawdown, at least 150 realizations along each pathway showed some effect from the pumping. Evidence for showing some effect from pumping is indicated here as having at least 1 mm of drawdown. The cumulative distributions of drawdown greater than 1 mm are shown for each pathway in Figure 5 and the data summarizing these results for each pathway are shown in Table 6.

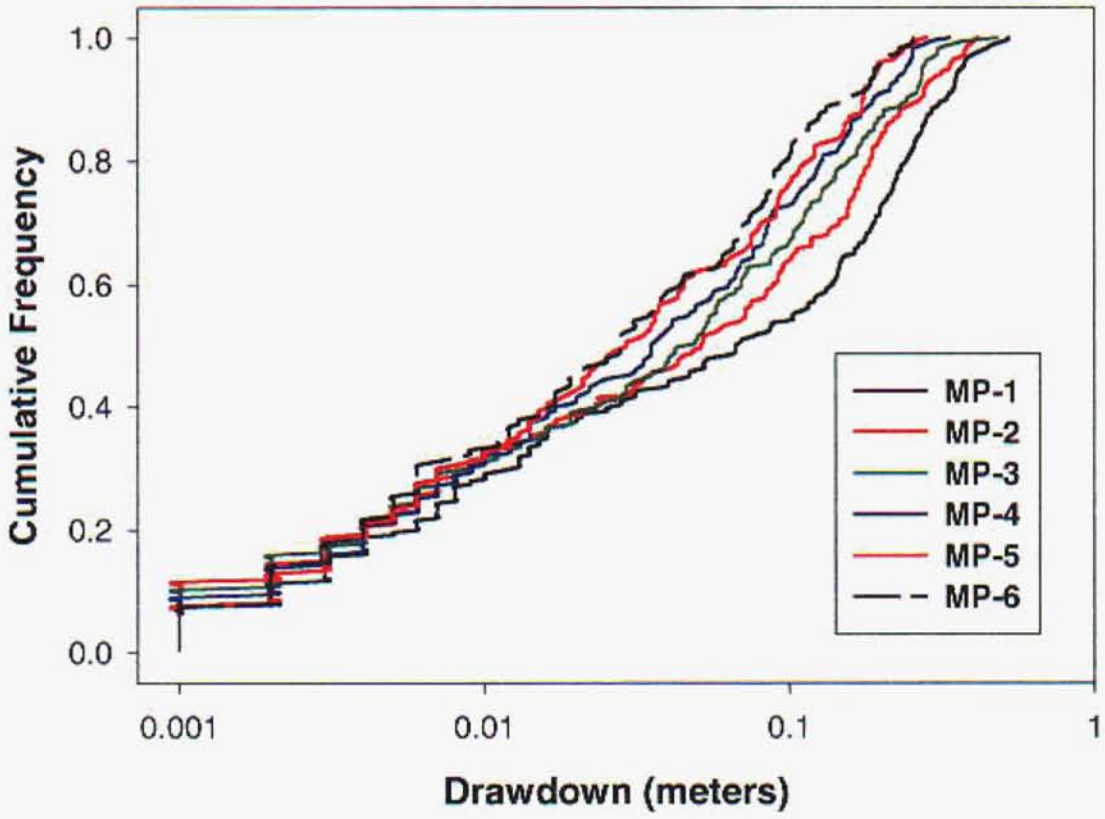

Figure 5. Cumulative distributions of drawdown after 12 days of pumping for all 6 piezometers. These results are for the radial flow conceptual model.

Table 6. Summary of results for the radial flow conceptual model.

Piezometer	Number Pumped	Number with >1mm Drawdown	Fraction of Pumped with > 1mm Drawdown	Number with > 1m Drawdown	Fraction of Pumped with > 1m Drawdown
MP-1	395	245	0.62	0	0.00
MP-2	395	219	0.55	0	0.00
MP-3	395	199	0.50	0	0.00
MP-4	395	179	0.45	0	0.00
MP-5	395	161	0.41	0	0.00
MP-6	395	153	0.39	0	0.00

Variable Flow Dimension Conceptual Model

The same distributions of K, S_s and L_p used in the calculation of drawdown with fully radial flow are used with a variable flow dimension between 1.0 and 2.0 to recalculate drawdown. As done in the radial flow case, 500 realizations are processed for each pathway. The cumulative distributions of drawdown after twelve days of pumping are shown in Figure 6. A summary of the results is provided in Table 7.

For the case of a variable flow dimension, a number of realizations in each pathway result in more than 1 meter of drawdown within the 12 day pumping period. These results are contrary to the results of the radial flow case where none of the 3000 realizations produced more than 1 meter of drawdown. The cumulative distributions of time necessary to achieve 1 meter of drawdown are given in Figure 7. The total number of realizations that could be pumped, the number of realizations resulting in any drawdown and the number of realizations resulting in more than 1 meter of drawdown are given in Table 7 for each piezometer. It is noted that even though some of the models showed caused the pumping well to go dry, it was possible to obtain more than one meter of drawdown in the piezometers with these models prior to pumping the pumping well dry.

Table 7. Summary of results for the variable flow-dimension conceptual model.

Piezometer	Number Pumped	Number of vectors with > 1mm Drawdown	Fraction of all 500 vectors with > 1mm Drawdown	Number Pumped with > 1m Drawdown	Fraction of Pumped with > 1m Drawdown
MP-1	180	293	0.59	140	0.78
MP-2	180	274	0.55	126	0.70
MP-3	180	255	0.51	111	0.62
MP-4	180	239	0.48	99	0.55
MP-5	180	217	0.43	80	0.44
MP-6	180	202	0.40	83	0.46

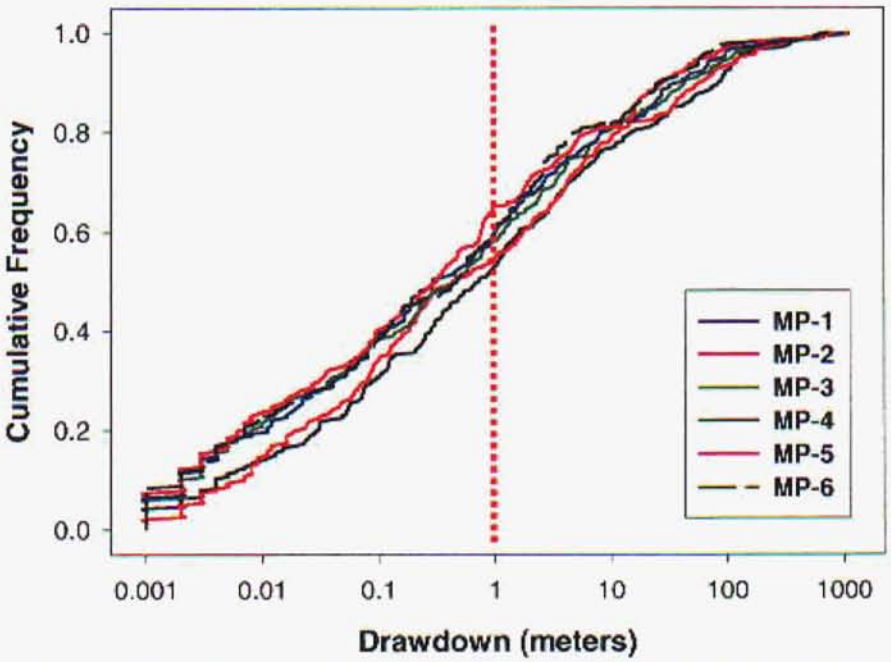

Figure 6. Cumulative distributions of drawdown after 12 days of pumping for all 6 piezometers in MIU-2. These results are for the variable flow-dimension conceptual model.

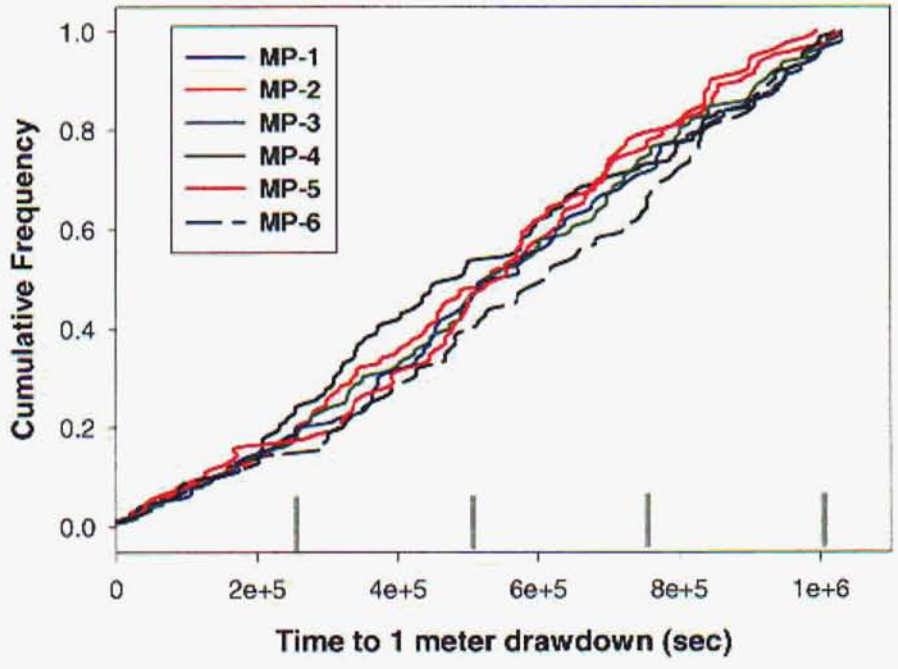

Figure 7. Cumulative distributions of the time necessary to achieve one meter of drawdown at the 6 piezometer locations in MIU-2. These results are for the variable flow-dimension conceptual model. The gray lines indicate the boundaries between the different steps in the pumping rate (three-day intervals).

Discussion

There are several notable differences between the results obtained with the flow dimension set to 2.0 and the case of the variable flow dimension. More of the input vectors can sustain the prescribed stepped pumping rate when the flow dimension is 2.0 than when the flow dimension is smaller. A total of 395 vectors were able to be pumped for 12 days without producing more than 777 meters of drawdown in MIU-3 for the case of the flow dimension equal to 2.0. Only 180 realizations could be pumped with less than 777 meters of drawdown in MIU-3 for the case of the variable flow dimension. A reduction in flow dimension can be thought of as a reduction in the cross-sectional area of flow towards the well. This reduction in flow area lowers the amount of discharge that can reach the pumping well relative to the radial flow case.

The larger cross-sectional flow area in the radial flow conceptual model limits the number of realizations that can produce 1 meter of drawdown within 12 days of pumping. In contrast, a total of 639 realizations (out of 3000) produce more than 1 meter of drawdown within 12 days of pumping when the flow dimension is less than 2.0 (compare the second column from the right-hand-side in Tables 6 and 7).

The sensitivity of the calculated drawdown to each of the uncertain input parameters is examined by graphing drawdown in the MIU-2 piezometers as a function of each input parameter (Figures 8, and 9). These figures combine together drawdown for all six MIU-2 piezometers. Keep in mind that for each piezometer location, it is only the path length that is different from the other piezometers (the same set of 500 K and S_s values were used across all six piezometer locations).

Figures 8 and 9 indicate several interesting features of the behavior of the fractured rock system as modeled here. The upper image in Figure 8 and the upper left image in Figure 9 show that as the log10 K value decreases below approximately -7, the corresponding value of drawdown in MIU-2 decreases rapidly. The minimum value of log10 K that produces a drawdown in MIU-2 is approximately -8.4, even though the distribution used in the modeling has values as low as -11.0.

The MIU-2 drawdown results are essentially independent of the specific storage values (see middle graph on Figure 8 and upper right graph in Figure 9). For both conceptual models, there is no correlation between the specific storage value and the resulting drawdown value.

Drawdown in MIU-2 is inversely proportional to the fracture path length for the radial flow conceptual model, (lower image of Figure 8), as would be expected. However this relationship is almost nonexistent for the variable flow-dimension conceptual model (Figure 9, lower left image) due the increased scatter caused by the variability in flow dimension.

In the case of the variable flow-dimension model, the drawdown in MIU-2 is most sensitive to the value of the flow dimension (lower right image, Figure 9). These results

appear to indicate that, for the parameters used in this modeling exercise, there is an upper bound on the amount of drawdown that can be achieved as a function of the flow dimension. At a flow dimension of 2.0 (the radial model) the maximum amount of drawdown is slightly less than 1 meter. This is the same result obtained for the radial conceptual model calculations in which the largest amount of drawdown across all realizations was 0.6 meters. The upper limit of drawdown increases to over 1000 meters for a flow dimension near 1.0.

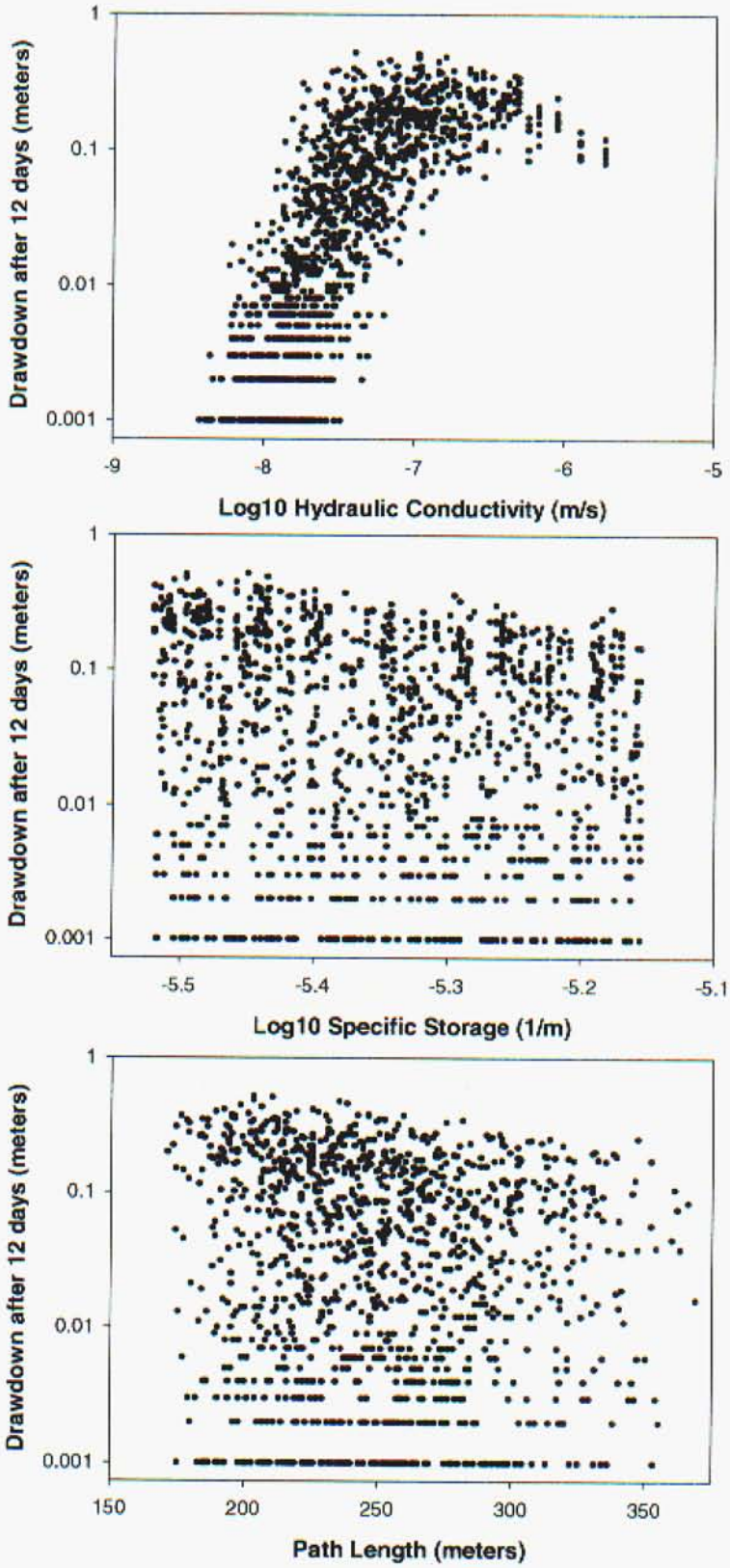

Figure 8. Drawdown after 12 days of pumping as a function of each of the three input parameters. These results are for the radial flow conceptual model.

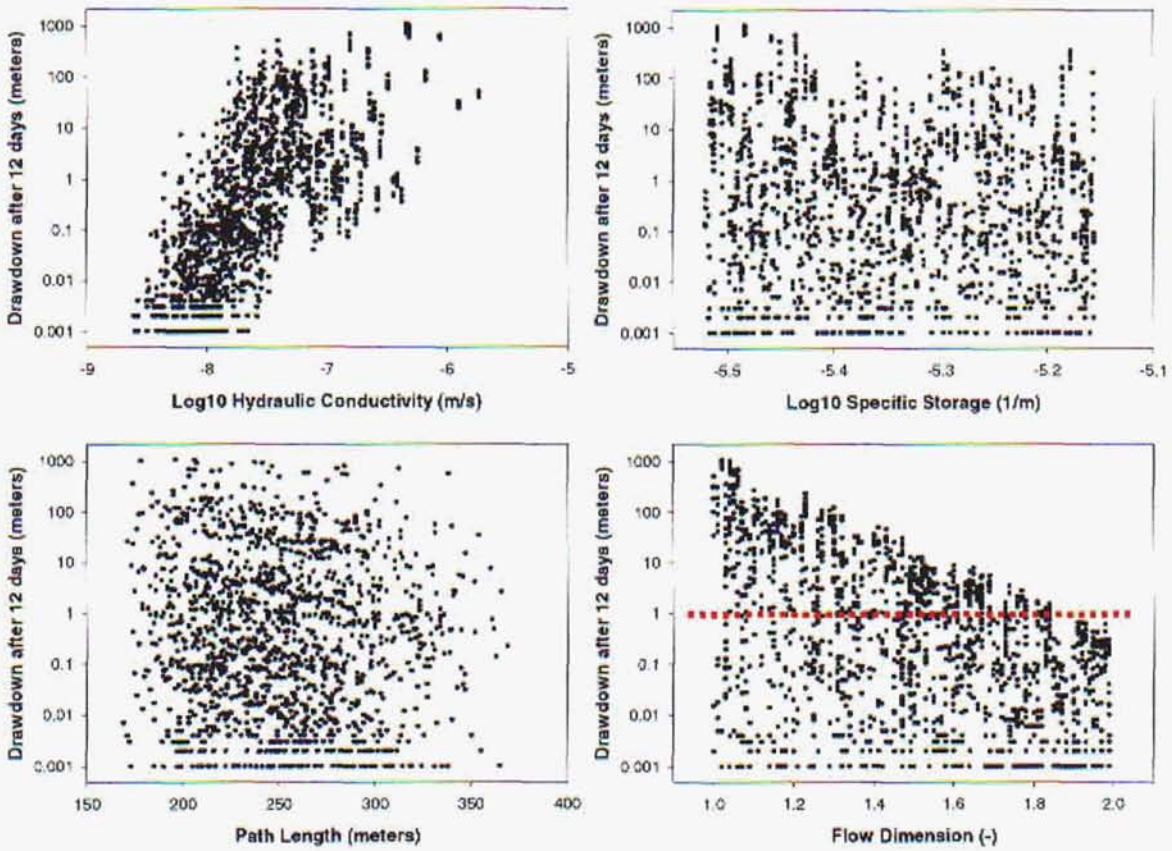

Figure 9. Drawdown after12 days of pumping as a function of each of the four input parameters. These results are for the variable flow-dimension conceptual model.

During presentation of these results at the TGC in late January, there was considerable discussion of the effects of the Tsukyoshi Fault on the results of the interference tests. The Tsukyoshi Fault was not modeled explicitly within these predictions of the interference tests. The conceptual model of the Tsukyoshi Fault is that of 10-meter thick, low permeability fault core surrounded by a highly fractured damage zone extending out for approximately 35 meters on each side of the fault core. The estimated hydraulic conductivity of the fault core is $1x10^{-09}$ (m/s) and the estimated hydraulic conductivity of the damage zone is $1x10^{-07}$ to $1x10^{-06}$ (m/s).

The sensitivity plots of hydraulic conductivity versus drawdown in Figures 8 and 9 can help answer the question of how the Tsukyoshi Fault will affect the interference tests. If the packers are arranged such that the interference test is conducted across the Tsukyoshi Fault (upper piezometers in Figure 1), then the average hydraulic conductivity of the pathway will be close to the fault core value of $1x10^{-09}$ (m/s). From the upper image in Figure 8 and the upper left image in Figure 9, there is a zero probability of observing 1 meter of drawdown in the MIU-2 piezometers for a pathway with an average hydraulic conductivity near $1.0x10^{-09}$ (m/s). However, if the interference test is conducted through the damage zone below the fault core (lower piezometers in Figure 1), then the average hydraulic conductivity of the pathway will be in the $1x10^{-07}$ to $1.0x10^{-06}$ (m/s) range.

Examination of the upper image of Figure 8 and upper left image of Figure 9 indicates a high probability of more than 1 meter of drawdown for a hydraulic conductivity in this high range associated with the damage zone of the fault.

Conclusions

Predictive modeling of drawdown for the interference tests being conducted between MIU-3 and MIU-2 indicates that calculated drawdown values are highly dependent on the flow dimension of the fracture system. If the fracture system produces water under radial flow conditions, the interference-testing program has a zero probability of success (see right-hand column of Table 6). However, we feel that representing the fracture system at the MIU site as an aquifer with a flow dimension less than 2.0 is a more realistic approach. Under these conditions, the probability for the success of the interference-testing program is considerably higher. However, it is noted that the probability of a hydraulic connection between MIU-3 and MIU-2 would be less in a system with near linear flow (flow dimension near 1.0) relative to a radial flow system (dimension near 2.0).

For the variable flow dimension case, the probability of exceeding 1 meter of drawdown within the 12 day pumping period for all 6 piezometers is given in the right hand column of Table 7. These probabilities range from 0.44 for the MP-5 piezometer to 0.78 for the MP-1 piezometer. These results show a inverse relationship with the minimum distances between the pumping interval and the piezometer location..

In practical terms, these results indicate a large probability of seeing more than1 meter of drawdown within 12 days along any pathway that is in the damage zone of the Tsukyoshi fault. For pathways that cross through the core of the Tsukyoshi fault, the probability of seeing more than 1 meter of drawdown in the piezometers is near zero. The probability of success for observing more than 1 meter of drawdown in all piezometers will increase if the pumping time and/or rate can be increased. However, there is a strong possibility that the drawdown in the MIU-3 borehole will reach the pumping interval if the pumping rate and/or pumping time are increased.

Reference

Domenico, P.A. and F.W. Schwartz, 1990, *Physical and Chemical Hydrogeology*, John Wiley and Sons, New York, 824 pp.